Nuclear Instruments and Methods in Physics Research A 338 (1994) 90–98
North-Holland

NUCLEAR INSTRUMENTS & METHODS IN PHYSICS RESEARCH
Section A

Can a gradient crystal compete with a mosaic crystal as a monochromator in neutron- or X-ray diffraction?

K.-D. Liss *, A. Magerl
Institut Laue – Langevin, F-38042 Grenoble Cédex, France

First a description of the Bragg reflection in polar coordinates is developed. Subsequently this formalism is applied to describe diffraction for mosaic crystals, gradient crystals and to include the Doppler effect on moving crystals. Within this framework the performance of a powder diffractometer as a two crystal configuration is evaluated. A traditional mosaic monochromator seems to be well suited when large values of reciprocal lattice vectors G are of main interest. However, a gradient crystal monochromator becomes competitive for $G^2/G^1 < 0.5$ with G^2 and G^1 representing the reciprocal lattice vectors of the sample and the monochromator, respectively. This holds in particular for a reflectometer, where the scientific interest focuses at small G^2 values. It is argued that particularly performant designs can be expected on a reflectometer for a monochromator which combines a reflection on a gradient crystal with a suitably chosen Doppler effect.

1. Introduction

In X-ray scattering beam definition is almost exclusively by reflection on single crystals. Although alternative techniques are employed occasionally in neutron scattering, still Bragg reflection represents the most widely used means to define the resolution and the performance of an instrument. Typical setups are e.g. powder diffractometers or reflectometers, where crystals appear at the monochromator- and at the sample position.

The monochromator uses the elastic mechanism of Bragg scattering by its lattice planes to define the condition of the wave impinging at the sample. On a powder diffractometer, the sample consists of a polycrystalline material. Differently oriented lattice planes satisfying their Bragg conditions reflect the incident wave into corresponding directions towards the detector. The separation of slightly different lattice parameters is limited by the angular resolution of the instrument. It depends on properties of the monochromator and in particular whether it is made from a gradient crystal or from a mosaic crystal. Further the orientation of the monochromator to the primary beam and the ratio of the lattice parameters of sample and monochromator play an important role for the resolution [1,2]. In the case of neutron scattering, the instrumental resolution can be further modified advantageously by the Doppler effect occurring by reflection on a moving crystal. This article will concentrate on a critical evaluation of these parameters.

A reflectometer is basically very similar to a powder diffractometer. However, the angle of incidence to the sample surface is in general restricted to less than say 5°. Hence, the interesting scattering vector $\boldsymbol{Q}$ perpendicular to the surface is typically less than 0.5 Å^{-1}.

Generally, perfect single crystals used as a monochromator deliver the best resolution. However the phase space element accepted by such a crystal is very small which results in lack of intensity. With well engineered phase space elements adapted to the particular scattering geometry and the interesting scattering components it is possible to increase the intensity by one to three orders of magnitude without suffering in resolution. Flat mosaic and gradient crystals as discussed here are two basic types of monochromator crystals which can be adapted for this purpose. Mosaic crystals consist of small crystallites where all corresponding reciprocal lattice vectors are oriented near a main direction within an angular distribution of approximately Gaussian shape. The characteristic mean value for this distribution function is called the mosaic spread η and it is defined by the full width at half maximum of this angular distribution. Note that the lengths of the $\boldsymbol{G}$ vectors for all mosaic blocks are identical.

While the mosaic spread for some materials like pyrolytic graphite cannot be reduced below certain values, research is conducted to induce appropriate

* Corresponding author.

SSDI 0168-9002(93)E0785-Q

mosaic spreads in other materials, e.g. Beryllium or Germanium. Typical values of the mosaic spread are in the range of $\eta \in [0, 2 \times 10^{-2}]$.

A gradient crystal is characterized by a variation of the length of its reciprocal lattice vectors $\boldsymbol{G}$ as a function of its spatial coordinates, while the directions of $\boldsymbol{G}$ are constant. The idea to use such crystals goes back to the early years of neutron scattering [3]. However, gradient crystals do not exist in nature and several research activities using temperature gradients [4], composition gradients [5] and acoustic wave gradients [6] are done to put them into the real world. The relative variation $\Delta G/G$ of the reciprocal lattice vector $\boldsymbol{G}$ is a characteristic property of the gradient crystal. It typically lies in the range $\Delta G/G \leq 10^{-3}$ and can rise for composition gradients up to several percent.

2. Bragg's law in polar coordinates

The basic mechanism for the reflection of a wave in a crystal is given by Bragg's law

$$\boldsymbol{k}_f = \boldsymbol{k}_i + \boldsymbol{G}, \quad k_f = k_i = k \tag{1}$$

where $\boldsymbol{k}_i$ and $\boldsymbol{k}_f$ are the incident and the scattered wave vectors, respectively, k represents their absolute value i.e. the wave number, and $\boldsymbol{G}$ is a reciprocal lattice vector. A more common representation is given with the introduction of the Bragg angle Θ by

$$\sin \Theta = G/2k. \tag{2}$$

In this section we recall the algorithm for the geometric construction of accepted and reflected wave vectors $\boldsymbol{k}_i$ and $\boldsymbol{k}_f$, under the condition that the length and the direction of a scattering vector $\boldsymbol{G}$ are given. Since Eq. (2) relates the wave number k with an angle, it seems that polar coordinates in reciprocal space are the natural and most convenient system for a graphical representation.

Let the incident white beam originate at the bottom of Fig. 1. It will then point to the origin O (zero line). Angles are measured from this line in the mathematical positive sense. The reciprocal lattice vector $\boldsymbol{G}$ is given in length and direction for an oriented crystal. For fixed $\boldsymbol{G}$ and given direction of the incident beam, $\boldsymbol{k}_i$ and $\boldsymbol{k}_f$ can be constructed in the following way: draw $\boldsymbol{G}/2$ from the origin. The perpendicular line AB with its mid point at the tip of $\boldsymbol{G}/2$ intersects the white beam at point A. The accepted wave vector $\boldsymbol{k}_i$ is given by

$$\boldsymbol{k}_i = \boldsymbol{AO}. \tag{3}$$

Since Bragg scattering is elastic, draw a circle with radius $\boldsymbol{k}_i$ around O. The intersection point B of the circle and the construction line gives the end point of the scattered wave vector

$$\boldsymbol{k}_f = \boldsymbol{OB}. \tag{4}$$

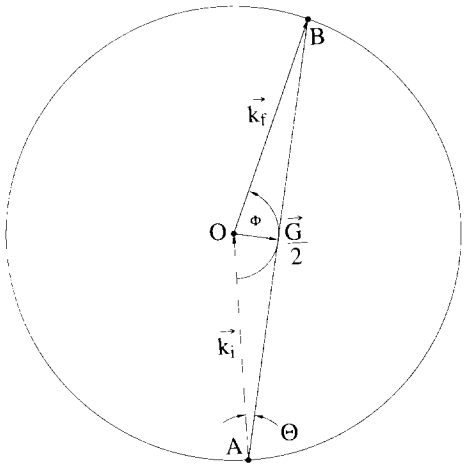

Fig. 1. Construction of the Bragg reflected and the accepted wave vectors $\boldsymbol{k}_f$ and $\boldsymbol{k}_i$, respectively, when the reciprocal lattice vector $\boldsymbol{G}$ is given. The white beam is incident from the bottom towards the origin O of the polar coordinate system. Φ and Θ are the orientation angle and the Bragg angle, respectively.

In our coordinate system, $\boldsymbol{k}_f$ is defined by the parameter pair (Φ, k), i.e. the absolute value of k and its orientation angle Φ. Thus $\boldsymbol{k}_f$ can be understood as a parametric function of k, Φ and $\boldsymbol{G}$ such that

$$\Phi = \Phi(k, \boldsymbol{G}). \tag{5}$$

From Eq. (2) and

$$\Phi = \pi - 2\Theta \tag{6}$$

follows

$$\Phi(k, \boldsymbol{G}) = \pm 2 \arccos(G/2k). \tag{7}$$

The positive and negative sign represent positive and negative orientations of $\boldsymbol{G}$, respectively.

2.1. Diffraction on a mosaic crystal

In case of a mosaic crystal the scattering vector $\boldsymbol{G}$ is rotated around the origin while its absolute value G remains constant. Thus the end points of scattered wave vectors lie on a curve with the parametric representation

$$\Phi(k) = \pm 2 \arccos(G/2k), \quad k \in [G/2, \infty]. \tag{8}$$

The two branches designed with + and − in Fig. 2 represent positive or negative orientations of $\boldsymbol{G}$. The accepted fraction of this curve depends on both the orientation of the average $\boldsymbol{G}$ vector and the mosaic spread η of the reflecting crystal. Minimal and maximal wave numbers k^- and k^+ belonging to $\boldsymbol{k}_f^-$ and $\boldsymbol{k}_f^+$

from Fig. 2 are selected by maximal and minimal Bragg angles,

$$\Theta^- = (\Theta + \eta/2), \tag{9a}$$

$$\Theta^+ = (\Theta - \eta/2), \tag{9b}$$

respectively. For a small mosaic spread η and avoiding a backscattering geometry with $\Theta = 90°$, the logarithmic derivative of Eq. (2) gives to a first order approximation:

$$\Delta k/k = \cot\Theta\, \Delta\Theta, \tag{10}$$

with $\Delta k = k^+ - k^-$ and $\Delta\Theta = \eta$. The reflected wave vectors fall into an angular interval $[\Phi(k^-), \Phi(k^+)]$ which means that the incident parallel beam is reflected into a divergent one. The divergence is given by

$$\Delta\Phi = \Phi(k^+) - \Phi(k^-). \tag{11}$$

Together with Eqs. (2), (7) and (9) we obtain

$$\Delta\Phi = 2\eta. \tag{12}$$

The geometric interpretation of this result is the fact that a reflected beam is deviated twice the rotation angle of the scattering vector.

2.2. Diffraction on a gradient crystal

A gradient crystal has a fixed orientation G/G of its reciprocal lattice vector distribution G but a variation in length $G \in [G^-, G^+]$. Thus all accepted wave vectors are reflected at the same angle

$$\Phi(k) = \text{const.}, \tag{13}$$

i.e. a gradient crystal reflects within its acceptance like an optical mirror (Fig. 3). In particular, there is no beam divergence induced by the reflection:

$$\Delta\Phi = 0. \tag{14}$$

The accepted interval $[k^-, k^+]$ is given again by the logarithmic derivative of Bragg's law. With G variable and Θ constant this gives

$$\Delta k/k = \Delta G/G. \tag{15}$$

with $\Delta k = k^+ - k^-$ and $\Delta G = G^+ - G^-$.

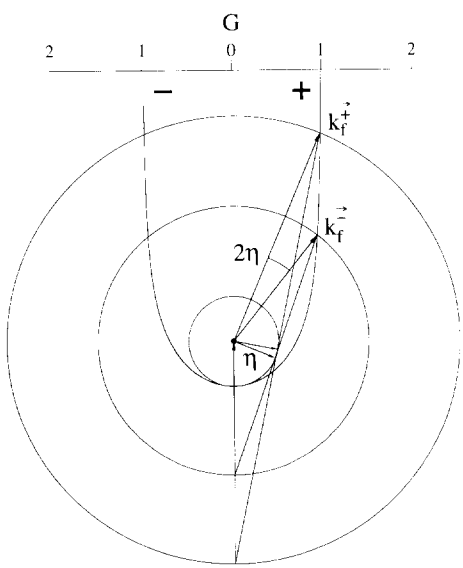

Fig. 2. Bragg reflection on a crystal with mosaicity η: Wave vectors of different lengths are reflected to k_f^- and k_f^+. Their end points are on the curved line from (−) to (+). A scale in units of the reciprocal lattice vector G is positioned at the top of the figure.

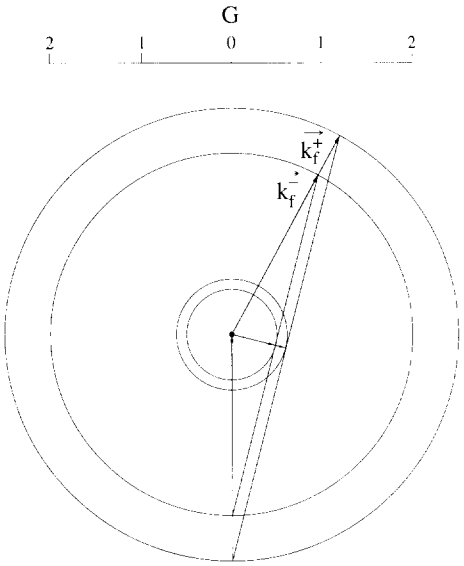

Fig. 3. Bragg reflection on a gradient crystal: The reflection takes place on a radial distribution of reciprocal lattice vectors resulting in a radial distribution of scattered wave vectors. Minimal and maximal wave vectors k_f^- and k_f^+ are selected depending on the gradient.

3. Diffraction on moving crystals

In addition to the previous chapters, the Doppler effect occurring by a reflection on a moving monochromator can be used to shape the reflected phase space element for the scattering conditions at the sample [7,8]. This mechanism provides for a large variety of phenomena. We concentrate here only on the basic construction rules and on some specific examples. Since the crystal velocity v_c has to be compared with the phase velocity of the considered wave, Doppler effects are negligible in the case of X-ray scattering, and the

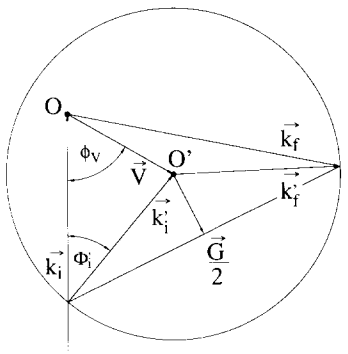

Fig. 4. Reflection on a moving crystal. The basic construction representing a Bragg reflection is done in a primed coordinate system with origin O'. It is shifted by V towards the system at rest with origin O. Wave vectors are scattered by G from k'_i to k'_f in the moving system. Since they have to be read from O in the system at rest, k_i and k_f have different lengths, and the scattering becomes inelastic.

following considerations only apply to neutron scattering.

The crystal velocity v_c in the laboratory system transforms like

$$V = \frac{m_n}{\hbar} v_c \tag{16}$$

into the reciprocal space of wave vectors. As usual m_n denotes the neutron mass and $\hbar$ Planck's constant. Since V is given, the construction of accepted and scattered wave vectors has to be performed in a primed coordinate system which is shifted by V from the system at rest. In Fig. 4, the origin O of the system at rest, in which all beam properties are measured, is shifted to the moving origin O' where the scattering takes place. The construction in the crystal system as given by Eq. (7) has to be modified by subtracting an angular shift Φ'_i since the set of incident wave vectors k'_i with polar coordinates (Φ'_i, k'_i) in O' is no longer parallel. Depending on k'_i, Φ'_i is related by

$$k'_i \sin \Phi'_i = V \sin \phi_v, \tag{17}$$

to V, where (ϕ_v, V) are the polar coordinates of V.

One can see immediately from Fig. 4 that in general

$$k_i \neq k_f, \tag{18}$$

i.e. the scattering process is inelastic.

O' can be largely modified with respect to O when an appropriate crystal velocity V is applied. This gives the possibility to translate and rotate phase space elements selected by a mosaic or a gradient crystal or even by a perfect crystal reflecting a largely divergent beam to any desired position and orientation in reciprocal space. However, limits may be imposed by technical restrictions for the crystal motion. In section 6.2 this will be discussed for the case of a moving gradient crystal.

4. The influence of an incident beam divergence

In the previous chapters an incident beam with no divergence was assumed. This would correspond to zero intensity because the volume for such a phase space element vanishes. Therefore realistic beam divergencies have to be added to the construction.

4.1. In-plane divergence

A divergent beam can be described by its boundary rays, inclined to each other by the divergence angle α. In Fig. 5 the case for the reflection on a mosaic crystal at rest is demonstrated. The construction discussed above must be done independently for all points. Obviously the corresponding construction diagrams as shown in Fig. 2 are only inclined to each other by α, and all wave vectors in the accepted phase space element

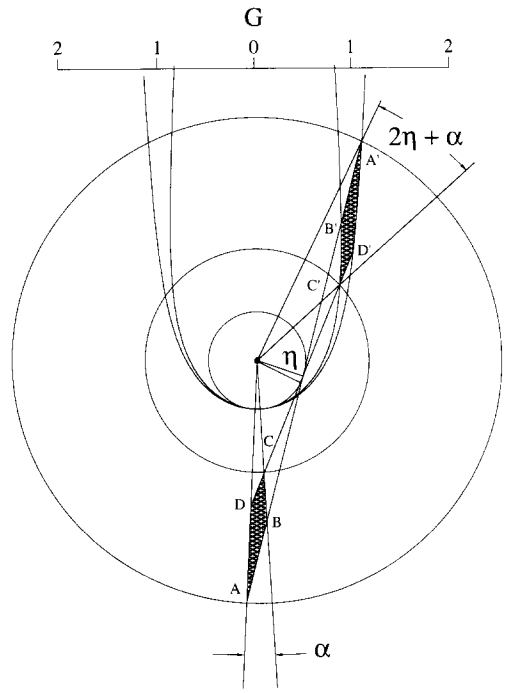

Fig. 5. Reflection on a mosaic crystal with mosaicspread η and an incident beam divergence α. The accepted phase space element $ABCD$ is scattered to $A'B'C'D'$. The construction can be done by considering the boundary beams AD and BC resulting in individual lines of end points $A'D'$ and $B'C'$ which are inclined to each other by α. The final divergence is $2\eta + \alpha$.

$ABCD$ are scattered to the reflected phase space element $A'B'C'D'$. The strength of the representation in polar coordinates is demonstrated again by the fact that the incident beam divergence α is simply an additive quantity to all angular dependencies. In particular the divergence of the reflected beam can be written as

$$\Delta\Phi(\alpha) = \Delta\Phi(\alpha = 0) + \alpha. \tag{19}$$

Thus it suffices for the following to study the case $\alpha = 0$ and considering Eq. (19) for the total beam divergencies, if necessary.

For the reflection on moving crystals, however, the influence of an incident beam divergence has to be treated in detailed cases which is not discussed in this paper. Generally, it results in a finite thickness of the phase space elements.

4.2. Out-of-plane divergence

For completeness, the basic diffraction properties for components perpendicular to the mean scattering plane are given in this chapter. In principle, the construction methods and results for crystals at rest are still valid: There is no additional beam divergence created by reflection on a gradient crystal since it reflects like an optical mirror. Thus, the total final divergence is given by Eqs. (14) and (19), where α has to be replaced by its vertical component β.

In the case of a mosaic crystal Eq. (12) has to be slightly modified by a projection. This gives

$$\Delta\Phi = 2\zeta \sin\Theta, \tag{20}$$

where ζ denotes the vertical component of the mosaic spread. For $\Theta \to 0$, $\Delta\Phi \to 0$, which is compatible with the fact that Bragg scattering on $G/k \to 0$ occurs like a point reflection. On the other side, for backscattering with $\Theta = 90°$, Eq. (20) becomes equal to Eq. (12), i.e. $\Delta\Phi = 2\zeta$. In this special geometry in-plane and out-of-plane scattering are no longer distinguished because the scattering plane degenerates to a line.

5. Two-crystal setups

So far the diffraction properties and the resulting beam divergencies for the reflection on one crystal, the monochromator, were discussed. This well defined beam can become incident onto another crystal, the sample.

In the following all quantities belonging to the first and second crystal are indexed by the superscripts 1 and 2, respectively. Quantities with no index are global. At the moment, we only consider scattering vectors of the same length $G^1 = G^2$ on both monochromator and sample. Let's assume for simplicity that the whole phase space element reflected by the monochromator is accepted by the sample.

The scattering vector $\boldsymbol{G}^2$ with an incident wave vector

$$\boldsymbol{k}_i^2 = \boldsymbol{k}_f^1, \tag{21}$$

must be aligned for a Bragg condition. For two dimensions, i.e. both scattering planes are parallel, there are two possible constellations for $\boldsymbol{G}^1$ to $\boldsymbol{G}^2$. In the dispersive $(++)$ case, $\boldsymbol{k}_i^1$ is rotated by a certain angle into $\boldsymbol{k}_f^1 = \boldsymbol{k}_i^2$ and then by the same angle in the same sense into $\boldsymbol{k}_f^2$. In the non-dispersive $(+-)$ case, $\boldsymbol{G}^2$ is antiparallel to $\boldsymbol{G}^1$, and $\boldsymbol{k}_i^2$ is rotated back by the negative angle into $\boldsymbol{k}_f^2$, which becomes parallel to $\boldsymbol{k}_i^1$ again.

Generally, the curve describing the end points of the scattered wave vectors can be written

$$\Phi(k) = \Phi^1(k) \pm \Phi^2(k), \tag{22}$$

the positive and negative sign representing the $(++)$ and $(+-)$ case, respectively. Then, the total beam divergence is given by

$$\Delta\Phi = \Phi(k^+) - \Phi(k^-), \tag{23}$$

where k^+ and k^- are the maximum and minimum wave numbers transmitted through the whole setup.

5.1. The mosaic–mosaic setup

Here we consider the two-crystal setup with mosaic crystals on both monochromator and sample positions. For the moment $G^1 = G^2$. The polar diagram for this

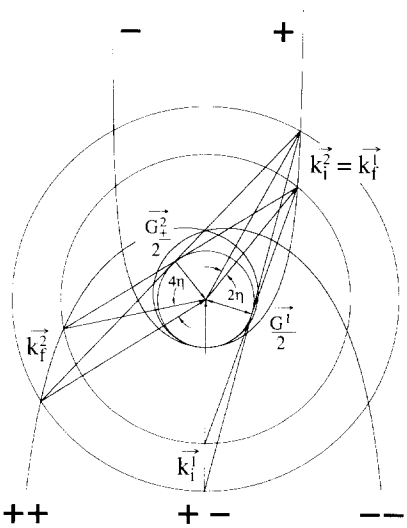

Fig. 6. Reflection on a mosaic–mosaic double crystal setup with $G^2 = G^1$ and mosaic spread η. Incident wave vectors $\boldsymbol{k}_i^1$ are scattered by $\boldsymbol{G}^1$ to $\boldsymbol{k}_i^2 = \boldsymbol{k}_f^1$. The second crystal scatters, depending on its orientation, either by $-\boldsymbol{G}^1$ back to $\boldsymbol{k}_f^2 = \boldsymbol{k}_i^1$ on the non-dispersive $(+-)$ branch or by $\boldsymbol{G}_+^2$ towards $\boldsymbol{k}_f^2$ on the dispersive branch from $(--)$ to $(++)$.

setup is given in Fig. 6. The incident wave vectors $\boldsymbol{k}_i^1$ are reflected by $\boldsymbol{G}^1$ within its acceptance interval into $\boldsymbol{k}_f^1 = \boldsymbol{k}_i^2$, falling with their end-points on the curve discussed earlier. In the (+ +) case the $\boldsymbol{k}_f^2$ vectors are ending on a curve with the parametric representation

$$\Phi(k) = 2\Phi^1(k), \tag{24}$$

because both scattering angles are identical in value and sense. $\Phi^1(k)$ is given by Eq. (8) and the final beam divergence with Eq. (12) becomes

$$\Delta\Phi = 4\eta. \tag{25}$$

In the (+ −) case, however, all wave vectors $\boldsymbol{k}_i^2$ are scattered by $\boldsymbol{G}^2 = -\boldsymbol{G}^1$ back into $\boldsymbol{k}_f^2 = \boldsymbol{k}_i^1$ and

$$\Phi(k) = 0. \tag{26}$$

Thus with Eq. (23)

$$\Delta\Phi = 0. \tag{27}$$

This is the best angular resolution possible. According to Eq. (19), it is equal to the incident beam divergence α.

Let us now consider $G^2 \neq G^1$. Similar curves for the wave vector end points can be calculated by applying Eq. (8) individually to the two reflections and putting the results into relations (22) and (23). Some examples are shown in Fig. 7. Again dispersive (+ +) and the non-dispersive (+ −) setups are different. The final direction of $\boldsymbol{k}_f^2$, given by Eq. (22) depends on both the wave number and the ratio G^2/G^1. Thus, the final beam divergence Eq. (23) becomes finite, even in the non-dispersive case.

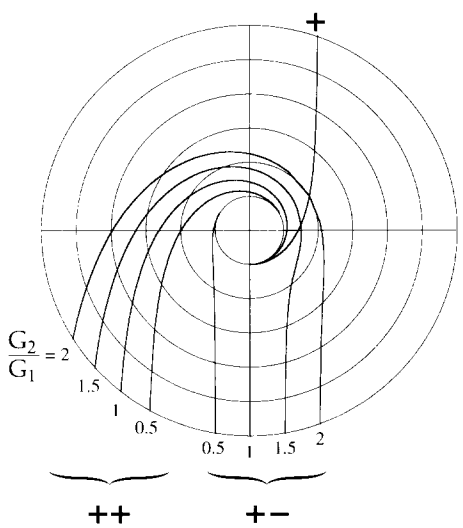

Fig. 7. Dispersive (+ +) and non-dispersive (+ −) branches for the lines of starting points of wave vectors passing through a double mosaic crystal setup and for different ratios G^2/G^1. The line of end-points (+) after the reflection on the first crystal is drawn from the zero line to the top of the graph.

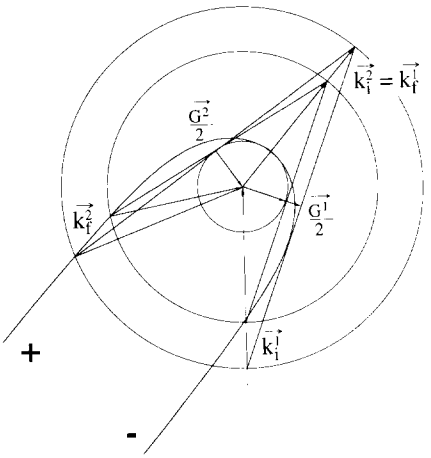

Fig. 8. Reflection on a gradient-mosaic double crystal setup. The first reflection occurs in analogy to an optical mirror where wave vectors are scattered by $\boldsymbol{G}^1$ from $\boldsymbol{k}_i^1$ to $\boldsymbol{k}_f^1$. The reflection at the mosaic crystal starts at $\boldsymbol{k}_i^2 = \boldsymbol{k}_i^1$ and it results from scattering on $\boldsymbol{G}^2$ to $\boldsymbol{k}_f^2$.

5.2. The gradient–mosaic setup

The case with a gradient crystal in the monochromator position and a mosaic sample is shown in Fig. 8. Then $\Phi^1(k) = \text{const.}$ and the resulting curve of end points is given by the reflection on one mosaic crystal, but rotated by Φ^1, i.e.

$$\Phi(k) = \Phi^1 \pm \Phi^2(k). \tag{28}$$

The accepted phase space element given by expression (15)

$$\Delta k/k = \Delta G^1/G^1 \tag{29}$$

is related through Eq. (10)

$$\Delta k/k = \cot\,\Theta^2\,\Delta\Theta^2 \tag{30}$$

to the angular dependencies. Thus

$$\Delta\Phi = 2\frac{\Delta G^1}{G^1}\tan\,\Theta^2\,\Delta\Theta^2 = 2\eta_{\text{eff}}. \tag{31}$$

A mosaic spread η_{eff} would give the same accepted phase space element than the gradient crystal. Note, however, that the reflected phase space elements would be very different in shape.

5.3. Discussion of double crystal setups

In the previous chapters, the angular resolutions for a double crystal diffractometer (powder diffractometer) with a mosaic or gradient crystal as a monochromator has been derived by simple geometric considerations in polar coordinates. The final beam divergencies $|\Delta\Phi|$ are given by Eq. (23) for both cases and they are plotted in Fig. 9 for several values of $\Theta^1 \in$

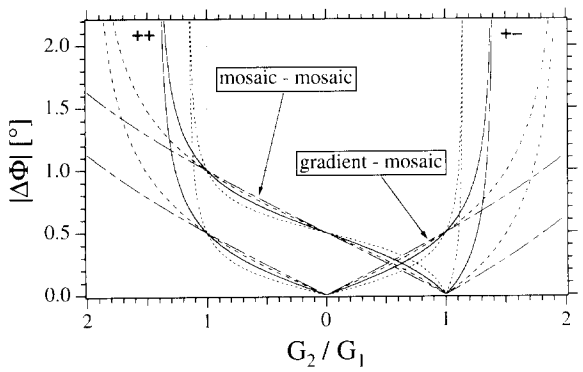

Fig. 9. Total beam divergencies $|\Delta\Phi|$ of wave vectors passing through a mosaic-mosaic or gradient–mosaic double crystal setup and plotted against the ratio G^2/G^1 of the reciprocal lattice vectors. Graphs for Bragg angles Θ^1 of 60°, 45°, 30° and 15° are given by dotted, continuous, short dashed and long-short dashed lines, respectively. The curves have been calculated for an effective mosaic spread of $\eta = 0.25°$. The solutions for the dispersive and the non-dispersive setups are distinguished on the left (+ +) and on the right (+ −) side, respectively.

{60°, 45°, 30°, 15°} and $\eta = \eta_{\text{eff}} = 0.25°$. The curves involving the gradient crystal have a minimum at $G^2 = 0$ and are symmetric on the (+ +) and (+ −) branches. The resolution for the mosaic case, however, is worse by 2η on the (+ +) branch and it reveals both an intersection with the resolution of the gradient case and a minimum at $G^2 = G^1$ on the (+ −) branch. Considering the limit $G^1 \to 0$ it can be shown by a simple point reflection in the polar diagram, that the point of intersection $G^2/G^1|_i$ of the two corresponding resolution curves is located at $G^2/G^1|_i > 0.5$. The upper limit is given by considering the backscattering geometry where $G^2/G^1|_i \to 1$. Generally, the intersection point lies in the interval $G^2/G^1|_i \in [0.5, 1]$.

In other words, a mosaic monochromator is very well suited for a traditional diffractometer where mostly $G^2 \gtrsim G^1$. Here the gradient crystal cannot compete. In the range $G^2/G^1 \in [0.5, 1]$, however, the performance of a gradient compared to a mosaic crystal becomes competitive and for $G^2/G^1 < 0.5$ the gradient case seems advantageous. This domain is of particular interest to fields of modern science like large scale structures in condensed matter, superlattices, artificial multilayers and magnetism.

We also note, that in the case of a gradient–mosaic setup both (+ +) and (+ −) branches are equivalent, whereas for the mosaic–mosaic setup the angular resolution is always better on the (+ −) branch.

6. The application to a reflectometer

In this chapter, we want to discuss two arguments related to the design of phase space elements for a reflectometer. The first demonstrates how to use an adequate distribution of reciprocal lattice vectors and the second refers to the powerful tool of the Doppler effect in the case of neutrons.

The main interest for reflectometers is to measure the component of the scattering vector $\boldsymbol{Q}$ perpendicular to a flat sample surface. Ideally, this implies an incident phase space element with a perpendicular component restricted to

$$\boldsymbol{\tau} = -\tfrac{1}{2}\boldsymbol{Q}, \tag{32}$$

for all wave vectors, whereas the components parallel to the surface may be extended over a wide distribution. In principle, such phase space elements are delivered by any perfect single crystal reflecting a divergent beam, and the problem would be an easy one if monochromator crystals with small enough reciprocal lattice vectors $\boldsymbol{G}$ matching the sample would exist. However, the difference of $\boldsymbol{G}$ vectors available by today's monochromator materials with the $\boldsymbol{Q}$ vectors to be measured is enormous, i.e. $G/Q \geq 10$. Artificial layered structures with well fitted $\boldsymbol{G}$ vectors could become a promising alternative as a monochromator on a reflectometer in the future.

6.1. Engineering arbitrary shapes of phase space elements

Using the two complementary tools based on longitudinal and transversal (angular) variations of the reciprocal lattice vectors it is possible to engineer any desired shape for the phase space element by reflection on an adequate distribution of reciprocal lattice vectors. For this end the correlation between the angular and the spatial distribution of $\boldsymbol{G}$ vectors has to be very well defined.

The construction designed for a reflectometer is illustrated in Fig. 10. $\boldsymbol{\tau}$ represents the component of the incident wave vectors $\boldsymbol{k}_i^2$ towards the sample, which is antiparallel to the sample scattering vector $\boldsymbol{Q}$ (Eq. (32)). An optimal distribution of the wave vectors is given by the line $R\tilde{R}$ which is perpendicular to $\boldsymbol{\tau}$. Their distribution can be projected back towards the incident white beam $\boldsymbol{k}_i^1$ which gives the distribution γ for the reciprocal lattice vectors $\boldsymbol{G}$.

A wave vector which originates in P must end in R. The half value of the corresponding scattering vector, $\boldsymbol{G}/2$, is given by the central point r of the section $[PR]$. The same construction can be done for the wave vector reflected from $\tilde{P}$ to $\tilde{R}$ resulting in $\tilde{r}$. The curve γ describing the whole $\boldsymbol{G}/2$ distribution can be obtained by continuing this construction for all the points of $R\tilde{R}$.

For an analytical solution, the straight line $R\tilde{R}$ is given by its polar coordinates (Φ, k) with

$$\Phi = \phi_\tau + \arccos(\tau/k), \tag{33}$$

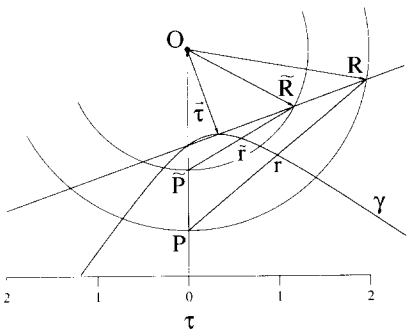

Fig. 10. Reconstruction of the distribution curve γ of reciprocal lattice vectors leading to a given reflected phase space element $R\tilde{R}$ in which all wave vectors have the same component τ. Wave vectors ending at $P(\tilde{R})$ originate from $P(\tilde{P})$. They have been scattered by a vector with its half value ending at point $r(\tilde{r})$ on γ.

Where (ϕ_τ, τ) denotes the coordinates of $\boldsymbol{\tau}$. When $\boldsymbol{G}$ is expressed by (ϕ, G), then its orientation is given by

$$\phi = \tfrac{1}{2}\Phi = \tfrac{1}{2}\{\phi_\tau + \arccos(\tau/k)\} \tag{34}$$

and the length distribution correlates by Eq. (7) to give

$$G = 2k \cos \phi. \tag{35}$$

The curve γ plotted in Fig. 10 has been calculated in this way.

This distribution of reciprocal lattice vectors could be realized by a lamella monochromator [9]. A gradient crystal has to be cut into slices along its gradient and each slice has to be inclined in accordance with its absolute value of its mean scattering vector.

6.2. Diffraction on a moving gradient crystal

In the following, it will be shown, that the desired phase space element for a reflectometer can be constructed using the transversal Doppler effect on moving gradient crystals.

The accepted phase space element near A in Fig. 11 is reflected by the gradient crystal towards B. The end points of the reflected wave vectors lie on a straight line BS which intersects the line of incidence AS at point S. The interesting $\boldsymbol{\tau}$ is defined by the perpendicular from the origin O to BS.

For the calculation of τ it is convenient to split the crystal velocity $\boldsymbol{V}$ into its components parallel and perpendicular to the reciprocal lattice vector $\boldsymbol{G}$:

$$\boldsymbol{V} = \boldsymbol{V}_\parallel + \boldsymbol{V}_\perp, \quad \text{with } \boldsymbol{V}_\perp \cdot \boldsymbol{G} \equiv 0. \tag{36}$$

ϕ is the orientation angle of $\boldsymbol{G}$ in the polar coordinate system, and $\measuredangle(ASO') = \phi$ and $\measuredangle(O'SB) = \phi$ with

$$\sin \phi = V_\perp / \overline{OS} \tag{37}$$

and

$$\sin 2\phi = \tau / \overline{OS}. \tag{38}$$

Combining these two relations gives

$$\tau = 2V_\perp \cos \phi. \tag{39}$$

Evidently τ depends only on the transversal Doppler component $V_\perp$, i.e. the velocity component parallel to the scattering crystal planes. The effect is most important for backscattering geometry where $\phi = 0$ and it vanishes in forward scattering geometry.

The principal information from a reflectometer relates to Q scans corresponding to a variation of τ. Eq. (39) implies that this can be done by varying $V_\perp$ alone. In this case the phase space element keeps its desired orientation parallel to the sample surface and it can be moved along $\boldsymbol{Q}$ with no loss in resolution.

As an example, $k = 2.5$ Å^{-1} is reflected from a Si[111] crystal ($G = 2.0$ Å^{-1}) and the (maximal) momentum transfer is $Q = 0.5$ Å^{-1}. This requires a (maximal) crystal velocity of $V_\perp = 0.31$ Å^{-1} or $v_c = 195$ m/s.

The reflection on a gradient crystal moving parallel to $\boldsymbol{G}$, i.e. $V_\perp = 0$ and $V_\parallel \neq 0$, is elastic. Then, the accepted phase space element is defined by an effective reciprocal lattice vector

$$\boldsymbol{G}_{\text{eff}} = \boldsymbol{G} + 2\boldsymbol{V}_\parallel, \tag{40}$$

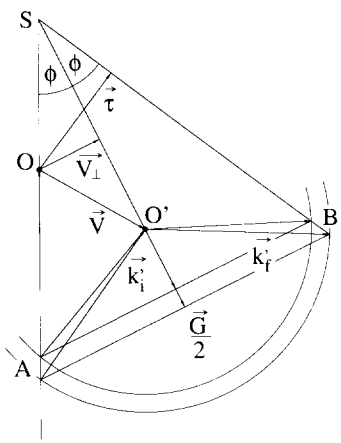

Fig. 11. The construction shown corresponds to a reflection on a gradient crystal moving with a velocity $\boldsymbol{V}$ suited for a reflectometer layout. All wave vectors ending near B all have the same component $\boldsymbol{\tau}$ with regard to the origin at rest O. Wave vectors $\boldsymbol{k}_i'$ are scattered by $\boldsymbol{G}$ into $\boldsymbol{k}_f'$. The accepted and reflected phase space elements are on straight lines AS and BS, respectively, which intersect the symmetry point S. According to the text τ can be expressed as a function of the orientation angle ϕ of $\boldsymbol{G}$ and the velocity component $V_\perp$ perpendicular to $\boldsymbol{G}$.

whereas its distribution width $\Delta G_{\text{eff}} = \Delta G$ remains constant, thus

$$\frac{\Delta G_{\text{eff}}}{G_{\text{eff}}} = \frac{\Delta G}{G \pm 2V_{\|}}. \tag{41}$$

Alternatively, one could imagine to use moving perfect crystals in a divergent beam for a reflectometer. Then an appropriate crystal velocity resulting in a small G_{eff} could provide an appropriate shape for the incident phase space element. For small Q, however, $V_{\|} \to G/2$ and the crystal velocity should be in the order of 630 m/s for a Si[111] reflection, which largely exceeds the above value for a gradient crystal.

However, the longitudinal Doppler effect is routinely applied on backscattering spectrometers [10,11], where a moving monochromator selects a neutron energy depending on its instantaneous velocity.

6.3. Results for the reflectometer

The comparison between gradient and mosaic crystal monochromators in section 5 clearly favors a gradient crystal for an application on a reflectometer. The resolution from its phase space element, however, becomes best for a sample scattering vector $\boldsymbol{Q} \to 0$. The ideal shape for the phase space elements and two construction methods have been demonstrated. The first method uses an adequate distribution of reciprocal lattice vectors to obtain the best resolution for a finite $\boldsymbol{Q}$. However, there remains the problem of scanning the Q range over one or two orders of magnitude while maintaining optimized conditions. This problem can be overcome easily by moving gradient crystals.

The reflectivity increases by a factor ν which is the ratio of the total ΔG to the natural width of reflection ΔG_{D} as given by the dynamical theory of diffraction [12,13]:

$$\nu = \Delta G / \Delta G_D. \tag{42}$$

Gradient crystals made by a $Si_{1-x}Ge_x$ composition gradient may theoretically rise to $\Delta G/G \leq 4 \times 10^{-2}$. However they are just entering into reality [14]. Gain factors of 10^3 can be expected with $\Delta G_{\text{D}}/G = 1.4 \times 10^{-6}$ for neutrons with $k = 2.5$ Å^{-1} and using the [220] reflection.

Looking for the angular divergence of the incident beam to the gradient crystal, it should be well collimated because it leads to a finite thickness of the phase space element and thus limits the resolution of the instrument.

7. Summary

A powerful method has been demonstrated to describe and to optimize the performance of crystal diffractometers. Starting from a description of the scattering process on one crystal (the monochromator), the treatment has been extended to double crystal setups, where the sample represents the second crystal. The estimated performance of monochromators made from gradient crystals or mosaic crystals depends on the scattering geometry and on the ratio of the scattering vectors at the monochromator crystal and at the sample. The Doppler effect has been considered as an additional and potentially very important degree of freedom to create optimized shapes of phase space elements. These considerations have been applied for the particular case of a neutron reflectometer, where a slim, but highly inclined resolution element is desirable.

References

[1] G. Caglioti, A. Paoletti and F.P. Ricci, Nucl Instr. and Meth. 3 (1958) 223.
[2] G. Caglioti and F.P. Ricci, Nucl. Instr. and Meth. 15 (1962) 155.
[3] H. Maier-Leibnitz and F. Rustichelli, Patentschrift 1816542, Deutsches Patentamt (1968).
[4] B. Alefeld, Z. Physik 228 (1969) 454.
[5] F. Rustichelli, in: Neutron inelastic scattering (International Atomic Energy Agency, Vienna, 1972) p. 697.
[6] R. Hock, T. Vogt, J. Kulda, Z. Mursic, H. Fuess and A. Magerl, Z. Physik B 90 (1993) 143.
[7] C.G. Shull, K.R. Morash and J.G. Rogers, Acta Crystall. A 24 (1968) 160.
[8] C.G. Shull and N.S. Gingrich, J. Appl. Phys. 35(3) (1963) 678.
[9] H. Maier-Leibnitz, Ann. Acad. Sci. Fennicae A. VI. 267 (1967) 1.
[10] A. Heidemann and J. Scholz, Z. Physik 263 (1973) 291.
[11] B. Alefeld, T. Springer and A. Heidemann, Nucl. Sci. Eng. 110 (1992) 84.
[12] H. Rauch and D. Petrascheck, AIAU 74405b, Atominstitut der Österreichischen Universitäten (1976).
[13] H. Rauch and D. Petrascheck, in: Neutron Diffraction, ed. H. Dachs, (Springer, Berlin/Heidelberg/New York, 1978) p. 303.
[14] R. Madar, E. Mastromatteo, A. Magerl, K.-D. Liss and C. Bernard, Surface and Coatings Technology 54 & 55 (1992) 229.